Human Molecular Genetics, 2001, Vol. 10, No. 5 477–484

WFS1 (Wolfram syndrome 1) gene product: predominant subcellular localization to endoplasmic reticulum in cultured cells and neuronal expression in rat brain

Koumei Takeda[1,+], Hiroshi Inoue[1,+], Yukio Tanizawa[1], Yumiko Matsuzaki[2], Jun Oba[2], Yoshifumi Watanabe[3], Koh Shinoda[2] and Yoshitomo Oka[1,§]

[1]Third Department of Internal Medicine, [2]Department of Anatomy, and [3]Department of Neuropsychiatry, Yamaguchi University School of Medicine, Ube, Yamaguchi 755-8505, Japan

Received 20 October 2000; Revised and Accepted 29 December 20000 DDBJ/EMBL/GenBank accession no. AF136378

Wolfram (DIDMOAD) syndrome is an autosomal recessive neurodegenerative disorder accompanied by insulin-dependent diabetes mellitus and progressive optic atrophy. Recent positional cloning led to identification of the *WFS1* (Wolfram syndrome 1) gene, a member of a novel gene family of unknown function. In this study, we generated a specific antibody against the C-terminus of the WFS1 protein and investigated its subcellular localization in cultured cells. We also studied its distribution in the rat brain. Biochemical studies indicated the WFS1 protein to be an integral, endoglycosidase H-sensitive membrane glycoprotein that localizes primarily in the endoplasmic reticulum (ER). Consistent with this, immunofluorescence cell staining of overexpressed WFS1 showed a characteristic reticular pattern over the cytoplasm and overlapped with the ER marker staining. No co-localization of WFS1 with mitochondria argues against an earlier clinical hypothesis that Wolfram syndrome is a mitochondria-mediated disorder. In the rat brain, at both the protein and mRNA level, WFS1 was found to be present predominantly in selected neurons in the hippocampus CA1, amygdaloid areas, olfactory tubercle and superficial layer of the allocortex. These expression sites, i.e. components of the limbic system or structures closely associated with this system, may be involved in the psychiatric, behavioral and emotional abnormalities characteristic of this syndrome. ER localization of WFS1 suggests that this protein plays an as yet undefined role in membrane trafficking, protein processing and/or regulation of ER calcium homeostasis. These studies represent a first step toward the characterization of WFS1 protein, which presumably functions to maintain certain populations of neuronal and endocrine cells.

INTRODUCTION

Wolfram (DIDMOAD) syndrome (OMIM 222300) is an autosomal recessive neurodegenerative disorder associated with juvenile-onset diabetes mellitus, progressive optic atrophy, sensorineural deafness and diabetes insipidus (1). The prognosis is poor and most patients die prematurely with severe neurological disabilities including organic brain syndrome and bulbar dysfunction (2). Neuropathological studies have shown diffuse neurodegenerative changes in the brain (3–5).

We recently succeeded in cloning the gene responsible for this disorder and designated it *WFS1* (Wolfram syndrome 1) (6). The gene encodes an 890 amino acid protein, presumably a transmembrane protein based on its secondary structure. No related genes have been found, however, in public databases, suggesting that *WFS1* is a member of a novel gene family. Mutation screening analysis of six Wolfram families showed a series of different mutations, including stop, frameshift, deletion and missense mutations (6). Thus, we speculate that loss-of-function mutations in this gene are responsible for Wolfram syndrome. Since our initial identification of the *WFS1* gene, more than 50 distinct mutations of this gene have been found by our research group and other investigators (H. Inoue *et al.*, unpublished data; 7–9).

Although analyses of the amino acid sequence of the WFS1 protein have revealed several structural domains, the physiological function of this protein remains totally unknown. WFS1 does not contain any leader sequences that target this protein to specific intracellular organelles. We noticed a region (amino acids 393–402) of human WFS1 (hWFS1) with sequence homology to the prenyltransferase α subunit repeat structure (6). This region is, however, unlikely to represent a targeting motif; the repeat signature is found only once in WFS1 protein, whereas it is found to be repeated five times in all known protein prenyltransferase α subunits. It was hypothesized that WFS1 is a nuclear encoding mitochondrial protein (10), since most of the clinical phenotypes characteristic of this syndrome are consistent with defects of mitochondrial function that are seen in mitochondrial diseases, such as MELAS, Leber's hereditary optic neuropathy (LHON) and maternally inherited diabetes and deafness (mitochondrial diabetes).

[+]These authors contributed equally to this work
[§]To whom correspondence should be addressed. Tel: +81 836 22 2250; Fax: +81 836 22 2256; Email: oka-y@po.cc.yamaguchi-u.ac.jp

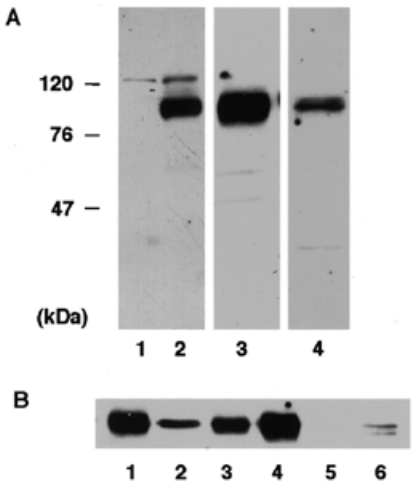

Figure 1. Immunoblot analysis of WFS1 protein. Cell lysates were subjected to SDS–PAGE (7.5% acrylamide gels) and western blot analysis was carried out using anti-WFS1C antibody. The molecular weight markers are shown to the left. (**A**) Anti-WFS1C antibody detected a 100 kDa band in the crude lysate of COS-7 cells transfected with the pcDNA3–hWFS1 (lane 2). Lane 1 represents the control COS-7 cell lysate without transfection. Anti-WFS1C antibody recognized intrinsic WFS1 protein in microsome fraction proteins (20 µg) from rat brain (lane 3) and human primary fibroblasts (lane 4). (**B**) Intrinsic WFS1 protein was detected in crude lysates (20 µg) of cultured cell lines: lane 1, human fibroblast; lane 2, HL-60; lane 3, HEK293; lane 4, HepG2; lane 5, PC12; and lane 6, COS-7. Note that the intrinsic WFS1 amount in COS-7 cells was very small. Although the WFS1 protein was not detectable in PC12 cells (lane 5) shown in this figure, longer exposure revealed its presence (data not shown).

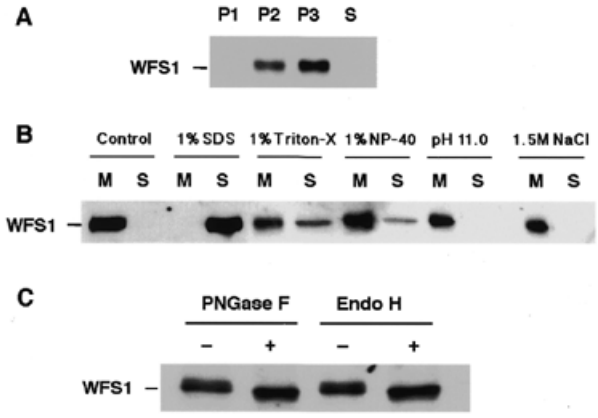

Figure 2. WFS1 is an integral membrane protein, localizing in ER to pre-Golgi. (**A**) Western analysis of crude organelles separated by differential centrifugation from human primary fibroblasts. P1, nuclear fraction; P2, mitochondria/microsome fraction; P3, microsome fraction; S, cytosol fraction. WFS1 is detected in the microsomal membrane-rich fractions (P2 and P3) but not the nuclear and cytosol fractions. (**B**) Treatment of the microsome fraction (P3) with detergents, alkaline and high salt. (**C**) Digestion of microsome fraction (P3) with either PNGase F or Endo H and following immunoblot analysis. The WFS1 immunoreactive band shows complete sensitivity to PNGase F and Endo H.

Supporting this hypothesis, heteroplasmic deletions of mitochondrial DNA have been observed in some Wolfram patients (11). Although a recent result obtained from the patients does not fit this hypothesis (12), no direct evidence has as yet been provided.

To address the potential functional role(s) of WFS1, we have conducted a series of experiments aimed at elucidating its subcellular localization in cultured cells and its distribution at both protein and mRNA levels in the rat brain.

RESULTS

Preparation and characterization of specific anti-WFS1 antibody

Two rabbits were immunized with glutathione *S*-transferase (GST) protein fused to the C-terminus of hWFS1 (GST–WFS1c). Characterization of the WFS1 antisera was performed using COS-7 cells transfected with a plasmid expression vector containing the full-length WFS1 cDNA (pcDNA3–hWFS1) as well as non-transfected cells. On SDS–PAGE and immunoblot analysis, one of these affinity-purified antibodies (anti-WFS1C) detected a prominent band migrating at ~100 kDa in the crude lysate of transfected cells (Fig. 1A, lane 2). The band size was consistent with the expected molecular mass of 100.29 kDa, predicted from the hWFS1 cDNA sequence. In addition, this protein band was specifically blocked by preincubation of the antibody with GST–WFS1c fusion protein (data not shown). These results suggest that the antibody specifically recognized WFS1 protein expressed in transfected COS-7 cells. A signal with the same molecular weight was also observed in non-transfected COS-7 cells, though at a much weaker level than in the transfected cells, indicating that the antibody also recognized endogenous WFS1 protein in COS-7 cells (Fig. 1A and B, lanes 1 and 6, respectively). Endogenous WFS1 protein was more clearly observed with anti-WFS1C antibody in primary human fibroblasts and rat brain extracts (Fig. 1A, lanes 3 and 4). This specific anti-WFS1C antibody was also used for detection of WFS1 protein in several mammalian cell lines. A relatively high level of endogenous WFS1 was observed in HepG2 cells, at an intermediate level in HK293 and HL-60 cells and at the lowest level in COS-7 and PC12 cells (Fig. 1B).

WFS1 is an integral membrane protein that localizes primarily in the endoplasmic reticulum (ER)

Human primary fibroblasts were used to characterize the subcellular localization of WFS1 protein. We first employed biochemical methods. Crude organelles were separated by differential centrifugation. Immunoblot analysis of the fractions revealed the presence of WFS1 protein in the microsome-enriched fractions (Fig. 2A, P2 and P3). Treatment of the microsome fraction (P3) with 1% SDS, 1% Triton X-100 or 1% Nonidet P-40 (NP-40) shifted the WFS1-specific immunoreactivity from the membrane to the supernatant fraction (Fig. 2B), although, under our experimental conditions, Triton X-100 and NP-40 treatments resulted in incomplete shifts. Treatment with 0.2 M Na_2CO_3, at pH 11.0 or 1.5 M NaCl, did not alter the membrane association of WFS1. Calnexin (p88) (13), known to be an ER transmembrane protein, responded to these manipulations in a fashion similar to that of WFS1 (data not shown). These results indicate that WFS1 is an integral membrane protein rather than a peripheral one.

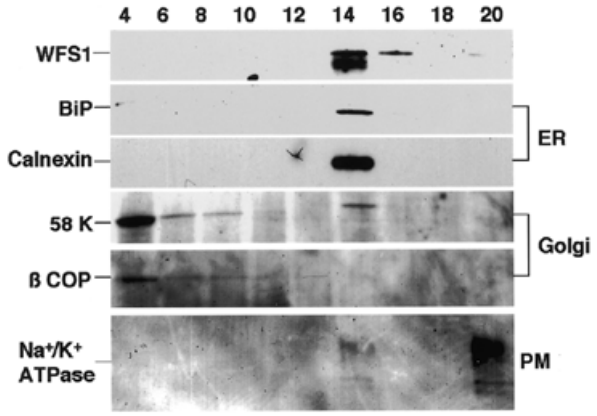

Figure 3. Subcellular distribution of WFS1. Subcellular fractions were prepared from human primary fibroblasts using iodixanol-based linear density gradient centrifugation. Nine representative fractions (fraction numbers are shown at the top of the panel) from the 20 collected were analyzed. Fraction 1 corresponds to the highest density and fraction 20 to the lowest density fraction. Fractions were analyzed by immunoblotting with antibody against the marker proteins for ER (BiP, calnexin), Golgi (58 K, βCOP) and plasma membrane (Na^+/K^+ATPase). WFS1 co-distributed with ER marker proteins.

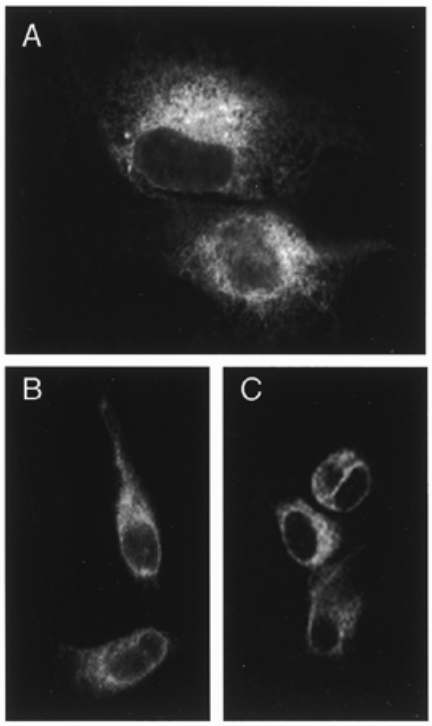

Figure 4. Immunocytochemical localization of WFS1 by confocal microscopy. Cells transfected with pcDNA3–hWFS1 were fixed and stained with anti-WFS1C antibody (1:200). Fluorescence images expressing WFS1 [(**A**) COS-7, (**B**) HeLa and (**C**) HepG2] were captured with a confocal image collection apparatus, using a 100× oil immersion lens.

Because the predicted secondary structure model of WFS1 allows for the existence of five putative Asn-glycosylation sites at amino acid positions 28, 335, 500, 661 and 746, we tested the *N*-glycosylation status of the WFS1 protein. Microsome fractions (P3) from primary fibroblasts were treated with PNGase F, an enzyme that cleaves N-linked oligosaccharides from proteins. Immunoblot analysis showed a shift in the electrophoretic mobility of WFS1 after PNGase F digestion (Fig. 2C). WFS1 was also sensitive to Endo H, an enzyme that cleaves all high-mannose oligosaccharides from proteins. Proteins that remain sensitive to Endo H are thought to be localized to the ER and *cis* portions of the Golgi (14). These findings indicate that WFS1 is a membrane protein, expressed predominantly in the ER.

In addition to a differential centrifugation method, we employed a refined fractionation method using 1–35% continuous iodixanol gradients. Fraction 14 was identified as an ER-rich fraction by immunoblot with an antibody against the well-characterized ER marker proteins BiP (GRP74) (13) and calnexin (Fig. 3). Golgi-rich fractions (58 K, βCOP) (15) and plasma membrane fractions (Na^+/K^+ATPase) corresponded to fractions 4–8 and 20, respectively. Immunoreactivity of the WFS1 protein was co-fractionated with ER marker proteins, but not with either Golgi or most of the plasma membrane marker proteins, confirming its predominant ER localization. A very small amount of Na/K ATPase was recovered in fraction 14. This may be due to minor contamination of this fraction by plasma membrane. It is also possible that a small amount of Na/K ATPase is derived from intracellular loci and/or that some WFS1 protein is present in the plasma membrane.

We also studied the subcellular localization of exogenously expressed hWFS1 using indirect immunofluorescence microscopy. Transient high-level expression of WFS1 was obtained in cell lines, COS-7, HeLa and HepG2, using a plasmid expression vector pcDNA3–hWFS1. Staining of COS-7 cells with anti-WFS1C antibody showed a characteristic reticular pattern over the cytoplasm and nuclear envelope (Fig. 4A). No apparent signals were detected in the plasma membrane. Similar results were obtained when WFS1 protein was expressed in HeLa and HepG2 cells (Fig. 4B and C). To further analyze the subcellular localization, double immunofluorescence analysis with subcellular organelle-specific dyes was performed (Fig. 5). The majority of WFS1 signals co-distributed with the signals of concanavalin A (16,17), which reportedly recognizes α-linked mannose or core oligosaccharides commonly found in ER (Fig. 5A–C). There were only minor overlapping signals with WGA (18), which binds to *N*-acetylglucosamine residues commonly added to membrane glycoproteins in the Golgi (Fig. 5D–F). No overlapping signals were observed with Mito-Tracker Red (19), a specific marker of mitochondria (Fig. 5G–I).

Neuronal expression of the WFS1 protein and mRNA in the rat brain

Since the brain is one of the major affected organs in Wolfram syndrome, it is highly plausible that the WFS1 protein is expressed in brain regions related to the neurological disabilities. Thus, the regional distributions of WFS1 protein and mRNA were examined in the rat brain by immunohistochemistry and *in situ* hybridization histochemistry, respectively. To generate a species-specific riboprobe for *in situ* hybridization studies, we cloned a rat homolog of the *WFS1* gene employing a dbEST database search and RT–PCR (GenBank accession no.

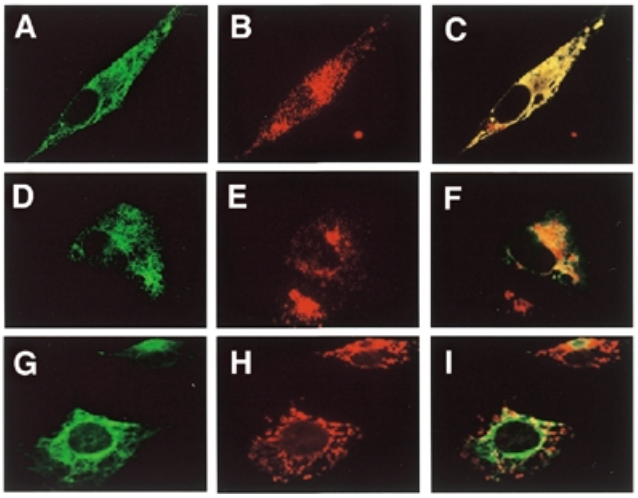

Figure 5. Co-localization of WFS1 and ER markers in COS-7 cells. Fluorescence images of COS-7 cells expressing hWFS1 (**A**, **D** and **G**) and the same cells co-stained with cell organelle-specific fluorescence markers [(**B**) Con-A/Texas Red (ER), (**E**) WGA/Texas Red (Golgi) and (**H**) Mito-Tracker Red (mitochondria)]. There is a large overlap between the green WFS1 signal and the red Con-A (ER) signal (**C**), producing the yellow signal. The green WFS1 signal shows a slight overlapping with the red WGA signal [Golgi (**F**)], whereas there is no overlapping with the red mitochondrial signal (**I**).

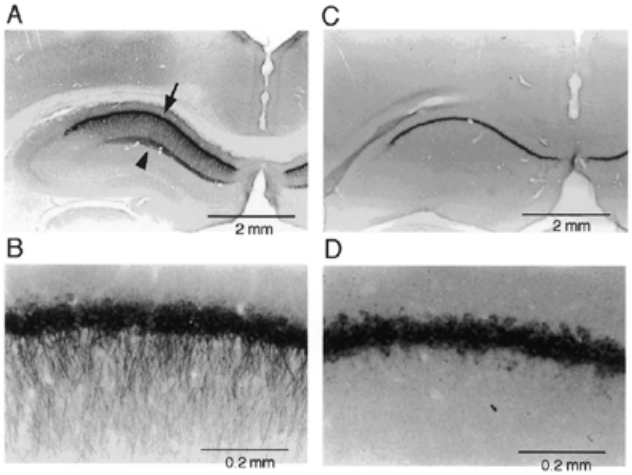

Figure 6. WFS1 protein (**A** and **B**) and mRNA (**C** and **D**) in the rat brain hippocampus. CA1 region pyramidal cells of Ammon's horn (arrow) are strongly positive for both the WFS1 protein and mRNA. The stratum lacunosum-moleculare of the CA1 region (arrowhead) is positive for the WFS1 protein but not for mRNA (C).

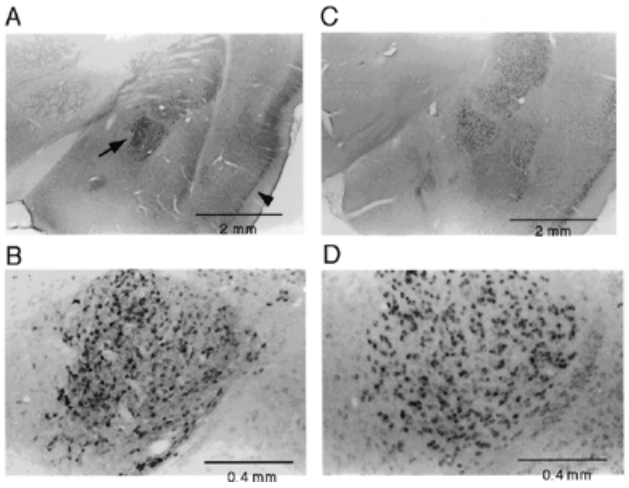

Figure 7. WFS1 protein (**A** and **B**) and mRNA (**C** and **D**) in the rat brain amygdala area. Arrow, the lateral subdivision of the central amygdaloid nucleus; arrowhead, the piriform.

AF136378). The rat coding sequence was 2673 bp in length and showed ~94 and 86% nucleotide identities, and 97 and 86% amino acid identities, with the mouse and hWFS1 sequences, respectively. The 1.55 kb fragment of rat WFS1 cDNA was subcloned into an RNA synthesizing plasmid and used for the synthesis of digoxigenin (DIG)-labeled mRNA antisense/sense probes.

Immunohistochemical analysis using the anti-WFS1C antibody demonstrated WFS1 immunoreactivity in a portion of neuronal cells in the forebrain, midbrain and lower brainstem, while no clear immunoreactivity was observed in glial cells. In immunopositive neurons, neuronal somata and proximal dendrites were strongly immunostained, showing a diffuse or reticular pattern, whereas distal dendrites, axons and axon terminals were only occasionally stained, showing a finer and more diffuse pattern (data not shown). No immunoreaction was detected when normal rabbit serum was used instead of the primary antibody.

The highest density of immunostaining in the brain was observed in the hippocampus, exclusively in CA1 region pyramidal cells of Ammon's horn (Fig. 6A, arrow, and B). Fine fibers or axon terminals of undetermined origins in the stratum lacunosum-moleculare of the CA1 region also showed marked WFS1 immunoreactivities (Fig. 6A, arrowhead). Immunoreactivity was specific in the CA1 region and was not detected in other cells in the dentate gyrus, CA2, CA3 or hilar regions of Ammon's horn, or in the adjacent subiculum. The results of *in situ* hybridization studies were consistent with those obtained by immunohistochemistry; WFS1 mRNA was present exclusively in CA1 region pyramidal cells of Ammon's horn, but not in other cells (Fig. 6C and D). The CA1 region signals were not observed with the sense probe (data not shown). In the cerebral cortex, a laminar distribution of WFS1-immunopositive neurons was observed throughout the second layer of the neocortex and the superficial layer of the allocortex, including the piriform (Fig. 7A, arrowhead), insular, perirhinal, cingulate and entorhinal cortices.

The amygdala area, especially neurons of the lateral subdivision of the central amygdaloid nucleus, showed a strong WFS1 immunoreactivity (Fig. 7A, arrow, and B). Again, the same regions were clearly positive in *in situ* hybridization studies (Fig. 7C and D). Moderate WFS1 immunoreactivity was also seen in neurons in the laterocaudal portions of the lateral amygdaloid nucleus, the posteromedial portion of the cortical amygdaloid nucleus, the posterior part of the basomedial

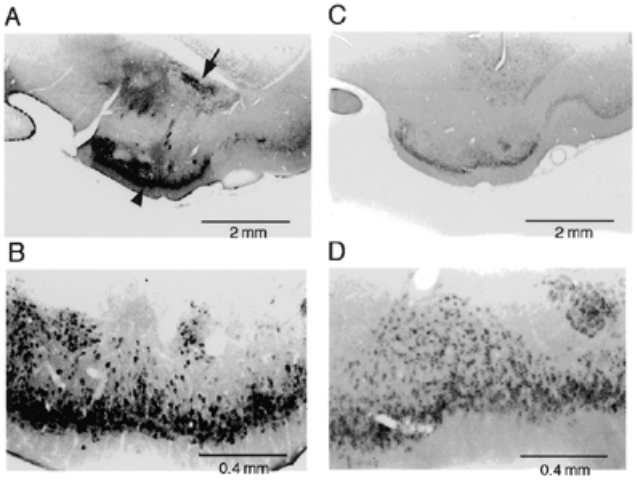

Figure 8. WFS1 protein (**A** and **B**) and mRNA (**C** and **D**) in the rat brain basal ganglia. Arrowhead, the olfactory tubercle; arrow, the posterior limb of the anterior commissure.

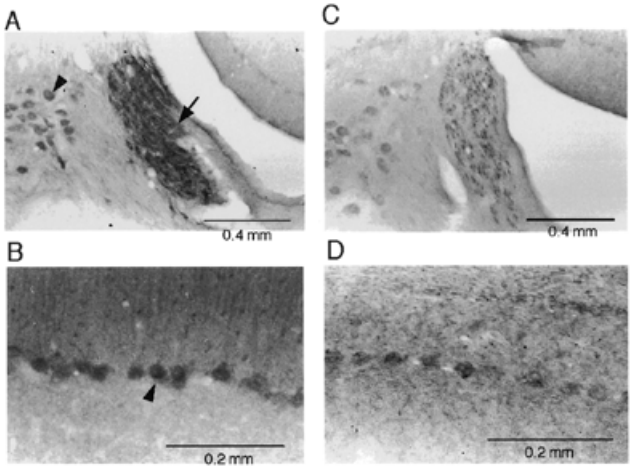

Figure 9. WFS1 protein (**A**) and mRNA (**C**) in the lower brainstem. Arrow, the locus coeruleus, arrowhead, the mesencephalic trigeminal nucleus. WFS1 protein (**B**) and mRNA (**D**) in the cerebellar cortex. Arrowhead, Purkinje cells.

amygdaloid nucleus, the intercalated cell mass, the amygdalopiriform transition area and the amygdalohippocampal transition area (data not shown).

In the basal ganglia, a strong WFS1 immunoreactivity was disseminated in neurons of the olfactory tubercle (Fig. 8A, arrowhead, and B) and the interstitial nucleus of the posterior limb of the anterior commissure (Fig. 8A, arrow). The immunopositive regions and the mRNA-positive regions (Fig. 8C and D) overlapped. Moderately immunoreactive neurons were distributed in the nucleus accumbens, amygdalostriatal transition area and medial margin of the caudate-putamen (data not shown).

Strongly WFS1-immunoreactive neurons were localized in the dorsal part of the lateral septal nucleus and the oval nucleus of the bed nuclear group of the stria terminals (data not shown). In the hypothalamus, moderately WFS1-immunoreactive neurons were present in the supraoptic nucleus and the lateral magnocular subdivision of the paraventricular nucleus. In the midbrain, a moderate level of WFS1 immunoreactivity was seen in the mesencephalic trigeminal nucleus (Fig. 9A, arrowhead) and in the transversely arrayed neurons that were distributed over the central nucleus of the inferior colliculus, the cuneiform nucleus, the oral part of the pontine reticular nucleus and the lateral lemniscus. In the lower brainstem, neurons in the locus coeruleus and subcoerular nucleus showed strong-to-moderate WFS1 immunoreactivities (Fig. 9A) and mRNA signals (Fig. 9C). Moderately immunoreactive neurons were seen in the motor trigeminal nucleus, the lateral vestibular nucleus, the facial nucleus, the ventral cochlear nucleus and the dorsal motor nucleus of the vagal nerve. Moderate immunoreacitivites were also found in the spinal nucleus of the trigeminal nerve, the pontine reticular formation and the gigantocellular or paragigantocellular nucelus (data not shown).

In the cerebellar cortex, Purkinje cells (Fig. 9B) and neurons in the medial, intermediate and lateral cerebellar nuclei showed moderate-to-weak WFS1 immunoreactivities, whereas no other cells in the cerebellar cortex were clearly immunostained. *In situ* hybridization studies showed the presence of WFS1 mRNA in Purkinje cells (Fig. 9D), although the signals were much weaker than those observed in the CA1 region of Ammon's horn.

DISCUSSION

Recently, we discovered *WFS1*, the gene responsible for Wolfram syndrome, using a positional cloning technique (6). This approach to gene discovery presupposes no knowledge of protein function, and the novel *WFS1* gene meets this criterion. Comparison of the amino acid sequence of *WFS1* with those in public databases revealed no related genes and no conserved sequence motifs, indicating that *WFS1* is likely to be a member of a new protein/gene family. In this study, to gain insight into the function of the WFS1 protein, we raised specific antisera directed against the C-terminal sequence of WFS1, which is highly conserved among mammalian species (human, mouse and rat).

With immunoblotting, endogenous WFS1 protein was detectable in extracts from rat brain and primary human fibroblasts, as well as in those from a variety of mammalian tumor cell lines tested. These results are consistent with our previous observations obtained by northern analysis (6), which demonstrated extensive expression of WFS1 mRNA in various tissues and cell lines. Thus, WFS1 is a ubiquitously expressed protein in many organs including the central nervous system. Intriguingly, however, in patients with the disease, only selected populations of neuronal and endocrine cells are affected.

The results of biochemical analysis indicate that WFS1 protein is an integral, endoglycosidase H-sensitive membrane glycoprotein. Supporting this hypothesis, immunofluorescence staining of WFS1 in cells showed staining patterns consistent with its ER localization. No evidence was obtained for co-localization of WFS1 with mitochondria. These observations strongly argue against an earlier clinical hypothesis that

Wolfram syndrome is a mitochondria-mediated disorder. The amino acid sequence of WFS1 lacks 'classical' sorting signals, such as the dilysine (KK)/diarginine (RR) and KDEL motifs (20), which reportedly sort proteins into the ER. However, not all ER-targeted proteins carry such sorting signals. Further investigation is needed to clarify the specific processes of sorting WFS1 to the ER membrane.

The ER localization of WFS1 suggests roles in membrane trafficking, protein processing and/or regulation of ER calcium homeostasis. Interestingly, in Wolfram syndrome patients with diabetes insipidus, abnormal processing of vasopressin precursor in the supraoptic and paraventricular nuclei was reported (21). Abnormal processing and modification of an unknown target protein may be associated with the development of other features of Wolfram syndrome. Recently, emerging data highlighted the importance of the ER as a regulatory site involved in cell death and apoptosis in neurodegenerative disorders. Presenilins (PS-1, -2), genes responsible for early-onset familial Alzheimer's disease, are ER membrane proteins (22). PS mutations lead to abnormal processing of β-amyloid precursor protein and increased production of amyloid β (Aβ)-peptide, resulting in increased vulnerability to apoptosis. Caspase-12, a newly identified member of the cysteine protease family, which consists of critical mediators of programmed cell death, was recently shown to localize to the ER (23). There it mediates an ER-specific apoptosis pathway and Aβ-peptide neurotoxicity. Because atrophy and selective cell defects of neurons and the endocrine system (e.g. pancreatic β-cells), which lack autoimmune and inflammatory process, are the most common morphological hallmarks of Wolfram syndrome (2), it is reasonable to speculate that an increased susceptibility to apoptosis in these cells/tissues may be involved in the pathogenesis of Wolfram syndrome. The hypothesis that WFS1 may function physiologically in a process protecting cells from an ER-specific apoptosis pathway is attractive, though more studies are needed to explore this possibility.

We also investigated the regional distributions of WFS1 protein and mRNA in the brain by immunohistochemistry and *in situ* hybridization histochemistry. Our results indicate that WFS1 is present in selected neurons at both the protein and the mRNA level. Notably, prominent expression was evident in the hippocampus, amygdala, olfactory tubercle and allocortex, i.e. components of the limbic system or structures closely associated with this system. These expression sites suggest that WFS1 may function in emotional, behavioral and visceral control. Indeed, psychiatric, behavioral and emotional abnormalities, such as depression, memory loss, assaultive behavior, anxiety and/or panic attacks, hallucinations and suicide attempts, are widely recognized as major clinical hallmarks of this disorder (24,25). It is of note that the severely affected regions in Wolfram syndrome patients do not necessarily correspond to the regions with high WFS1 protein levels; marked cerebellar atrophy is observed in the patients, despite WFS1 protein levels not being particularly prominent in the cerebellum compared with most other brain regions. The present studies were conducted in the rat brain, and species differences may exist. It is also possible, however, that additional factors intrinsic to the affected cells may facilitate the aforementioned apoptotic processes in conjunction with decreased WFS1 function. This hypothesis merits further investigation.

This study represents a first step towards the characterization of WFS1 protein. The precise role(s) of this protein remains to be elucidated. WFS1 presumably functions to maintain certain populations of neuronal and endocrine cells. Thus, discovery of its molecular function should greatly enhance our understanding of the mechanisms underlying various neurodegenerative disorders and diabetes mellitus.

MATERIALS AND METHODS

Cells, reagents and biochemicals

Primary human fibroblasts (CCD-1059Sk) were obtained from American Type Culture Collection (ATCC). The expression vectors pGEX-6X, pMAL-c2 and pcDNA3.1 were from Amersham Pharmacia Biotech, NEB and Invitrogen, respectively. Anti-BiP (GRP74) and anti-calnexin were from Stressgen, anti-βCOP and anti-58K from Sigma and anti-α1 subunit Na^+/K^+ATPase antibody from Affinity BioReagents.

Generation of the pcDNA3–hWFS1 construct

A hWFS1 cDNA fragment (nucleotides 159–2848, GenBank accession no. AF084481) was subcloned into the expression vector pcDNA3.1 and designated pcDNA3–hWFS1. Transfections were performed using LipofectAMINE (Life Technologies).

Preparation of anti-WFS1 antibody and western blots

The cDNA encoding the C-terminal 241 amino acids of hWFS1 was cloned into the pGEX-6X plasmid or pMAL-c2 plasmid, to produce chimeric proteins consisting of an N-terminal GST protein or maltose-binding protein (MBP) and the C-terminal sequence of WFS1 (GST–WFS1c and MBP–WFS1c, respectively). The GST–WFS1c chimeric protein was expressed in *Escherichia coli* (JM109), purified and used for immunizing Japanese White rabbits. Rabbit antisera were collected and affinity-purified using MBP–WFS1c. SDS–PAGE and immunoblotting were carried out as described previously (26).

Expression of hWFS1 in cultured cells and immunofluorescence microscopy

Cells transfected with pcDNA3–hWFS1 were re-plated on coverslips, fixed with 3.7% formaldehyde and permeabilized with 0.2% Triton X-100. Cells were incubated with anti-WFS1C antibody (1:200 dilution), then with secondary antibody [Alexa 488 goat anti-rabbit IgG (H+L) conjugate (1:500; Molecular Probes)]. Counterstaining of mitochondria was performed on living cells with Mito-Tracker Red (Molecular Probes). The ER and Golgi were stained on fixed cells with concanavalin A/Texas Red and WGA/Texas Red, respectively (Molecular Probes). Cells were visualized and photographed with a Zeiss LSM510 (version 2.01) confocal image collection apparatus, using a 100× oil immersion lens.

Subcellular fractionation of human fibroblasts and glycosylation analysis

Separation of crude organelles was performed on primary human fibroblasts using the differential centrifugation method (27). Cell lysates were fractionated into P1, nuclear fraction; P2, mitochondria/microsome fraction; P3, microsome fraction; and S, cytosol fraction. Microsome membrane extractions were prepared by treating the microsome fraction (P3) with 1% SDS, 1% NP-40, 1% Triton X-100, 1.5 M NaCl or 0.2 M Na_2CO_3, pH 11.0. Refined subcellular fractionation was performed using iodixanol (OptiPrep; Nycomed Pharma AS) linear gradients following the manufacturer's protocol. Twenty fractions (~600 µl each) were recovered by continuous elution from the bottom and subjected to SDS–PAGE, followed by immunoblotting analysis. For glycosylation analysis, cell lysates were treated with 750 U of peptide:*N*-glycosidase F (PNGase F) or endoglycosidase H (Endo H) at 37°C overnight in 25 µl of total reaction volume.

Immunohistochemical staining in rat brain

Rat brain sections were prepared and immunohistochemical analysis was performed as described previously (28). Briefly, 30 µm thick sections were incubated for 3 days at 4°C in 0.02 M PBS containing 0.05% normal goat serum and the affinity-purified anti-WFS1C antibody at a 1:1000 dilution, followed by incubation with biotinylated goat anti-rabbit IgG (1:500 dilution; Cappel) and peroxidase-conjugated streptavidin (1:500, Vector). For diaminobenzidine (DAB) staining, sections were reacted with 0.05 M Tris–HCl buffer containing 0.02% DAB, 0.6% nickel ammonium sulfate and 0.006% hydrogen peroxide. Sections were mounted onto glass slides, air-dried, dehydrated with a graded ethanol series, immersed in xylene and embedded in Entellan New (EMS).

EST search and cloning of rat WFS1 cDNA by RT–PCR

The dbEST database search was performed with an NCBI WWW server using the BLAST program. Primers for RT–PCR were designed from rat EST sequences (GenBank accession nos AI172032, AI407433 and AI044741), which were highly homologous to the hWFS1 cDNA sequence. Rat-specific PCR primers were as follows: RAT-U1, 5′-GTACCCCTTACACGCCATCAT-3′; RAT-L1, 5′-GAAGGACCTCACAGCAACAT-3′; RAT-L2, 5′-GAGGCCACGTCAATCAGGTA-3′. Because no rat EST sequences matched the N-terminal region of WFS1, an upper strand primer (MOUSE-U1: 5′-gcactgcggccggcaagATG-3′; lower case, 5′ untranslated region; underlined, translational start codon) was chosen based on mouse cDNA sequence. cDNA was synthesized from rat insulinoma (RIN) cell total RNA using SuperScript II and oligo(dT) primers (Gibco BRL). RT–PCR amplification was performed as described previously (29). The resulting PCR products were gel-purified and subcloned into pCR-Blunt vector and the inserts were sequenced from both orientations.

In situ hybridization in rat brain

To synthesize a riboprobe for *in situ* hybridization, the 1.55 kb fragment of rat WFS1 cDNA was amplified from RIN cells by RT–PCR, and subcloned into pCR-Blunt vector. The primers used were as follows: RAT-U2, 5′-TCCGTACTCTCACCGACCTG-3′ and RAT-L3, 5′-CTCAGGCGGCAGACAGGAAT-3′. Two independent clones containing the insert with a different orientation (pCR-clone19 for sense, pCR-clone1 for antisense) were chosen to generate DIG-labeled RNA probes using a T7 RNA polymerase with a DIG RNA labeling kit (Boehringer Mannheim). For *in situ* hybridization, adult rat brain paraffin sections (coronal and sagittal, 7 µm thickness) were prepared freshly as for immunohistochemical analysis. Sections were pretreated as follows: (i) dewaxing, rehydration and refixation; (ii) deproteination and acetylation; (iii) proteinase K treatment; and (iv) redehydration. Hybridization was performed for 12 h at 55°C in 50% formamide: 10 mM Tris–HCl pH 7.6, 1 mM EDTA pH 8.0, 600 mM NaCl, 1× Denhardt's solution, 10% dextran sulfate, 0.25% SDS, 200 µg/ml yeast tRNA, with diluted DIG–RNA probes. Following hybridization, the sections were washed and treated with 20 µg/ml RNase A in 10 mM Tris–HCl pH 7.6, 500 mM NaCl at 37°C. Sections were rinsed again and incubated for 1 h at room temperature with alkaline phosphatase-conjugated anti-DIG antibody (Boehringer Mannheim). Signals were visualized by incubating with BCIP/NBT substrate (DAKO) for 6–12 h at 37°C. The reaction was stopped with TE (10 mM Tris–HCl pH 7.6, 1 mM EDTA), and sections were mounted in Aqua-Poly/Mount (Polyscience).

Animal experiments

All experimental protocols were approved by the committee on the Ethics of Animal Experimentation at Yamaguchi University School of Medicine, and were conducted according to the guidelines for Animal Research of Yamaguchi University School of Medicine and The Law (No. 105) and Notification (No. 6) of the Japanese Government.

ACKNOWLEDGEMENTS

We would like to thank Ms Yukari Kora for her technical assistance. This work was supported by a grant from Kanae Foundation for Life and Socio-Medical Science (H.I.), a Grant-in-Aid for Creative Basic Research (10NP0201 to Y.O.) and Scientific Research (12357007 to Y.O. and 11557012 to Y.T.) from the Ministry of Education, Science, Sports and Culture of Japan.

REFERENCES

1. Barrett, T.G. and Bundey, S.E. (1997) Wolfram (DIDMOAD) syndrome. *J. Med. Genet.*, **34**, 838–841.
2. Barrett, T.G., Bundey, S.E. and Macleod, A.F. (1995) Neurodegeneration and diabetes: UK nationwide study of Wolfram (DIDMOAD) syndrome. *Lancet*, **346**, 1458–1463.
3. Shannon, P., Becker, L. and Deck, J. (1999) Evidence of widespread axonal pathology in Wolfram syndrome. *Acta Neuropathol. (Berl.)*, **98**, 304–308.
4. Genis, D., Davalos, A., Molins, A. and Ferrer, I. (1997) Wolfram syndrome: a neuropathological study. *Acta Neuropathol. (Berl.)*, **93**, 426–429.
5. Kinsley, B.T. and Firth, R.G. (1992) The Wolfram syndrome: a primary neurodegenerative disorder with lethal potential. *Ir. Med. J.*, **85**, 34–36.
6. Inoue, H., Tanizawa, Y., Wasson, J., Behn, P., Kalidas, K., Bernal-Mizrachi, E., Mueckler, M., Marshall, H., Donis-Keller, H., Crock, P. *et al.* (1998) A gene encoding a transmembrane protein is mutated in patients with diabetes mellitus and optic atrophy (Wolfram syndrome). *Nature Genet.*, **20**, 143–148.
7. Hardy, C., Khanim, F., Torres, R., Scott-Brown, M., Seller, A., Poulton, J., Collier, D., Kirk, J., Polymeropoulos, M., Latif, F. and Barrett, T. (1999)

Clinical and molecular genetic analysis of 19 Wolfram syndrome kindreds demonstrating a wide spectrum of mutations in WFS1. *Am. J. Hum. Genet.*, **65**, 1279–1290.

8. Strom, T.M., Hortnagel, K., Hofmann, S., Gekeler, F., Scharfe, C., Rabl, W., Gerbitz, K.D. and Meitinger, T. (1998) Diabetes insipidus, diabetes mellitus, optic atrophy and deafness (DIDMOAD) caused by mutations in a novel gene (wolframin) coding for a predicted transmembrane protein. *Hum. Mol. Genet.*, **7**, 2021–2028.
9. Gomez-Zaera, M., Storm, T., Meitinger, T. and Nunes, V. (1999) Wolframin mutations in Spanish families with Wolfram syndrome. *Am. J. Hum. Genet.*, **65** (suppl.), 1673.
10. Bu, X. and Rotter, J.I. (1993) Wolfram syndrome: a mitochondrial-mediated disorder? *Lancet*, **342**, 598–600.
11. Barrientos, A., Casademont, J., Saiz, A., Cardellach, F., Volpini, V., Solans, A., Tolosa, E., Urbano-Marquez, A., Estivill, X. and Nunes, V. (1996) Autosomal recessive Wolfram syndrome associated with an 8.5-kb mtDNA single deletion. *Am. J. Hum. Genet.*, **58**, 963–970.
12. Barrett, T.G., Scott-Brown, M., Seller, A., Bednarz, A., Poulton, K. and Poulton, J. (2000) The mitochondrial genome in Wolfram syndrome. *J. Med. Genet.*, **37**, 463–466.
13. Hebert, D.N., Simons, J.F., Peterson, J.R. and Helenius, A. (1995) Calnexin, calreticulin and Bip/Kar2p in protein folding. *Cold Spring Harbor Symp. Quant. Biol.*, **60**, 405–415.
14. Cai, Y., Maeda, Y., Cedzich, A., Torres, V.E., Wu, G., Hayashi, T., Mochizuki, T., Park, J.H., Witzgall, R. and Somlo, S. (1999) Identification and characterization of polycystin-2, the *PKD2* gene product. *J. Biol. Chem.*, **274**, 28557–28565.
15. Yamaji, R., Adamik, R., Takeda, K., Togawa, A., Pacheco-Rodriguez, G., Ferrans, V.J., Moss, J. and Vaughan, M. (2000) Identification and localization of two brefeldin A-inhibited guanine nucleotide-exchange proteins for ADP-ribosylation factors in a macromolecular complex. *Proc. Natl Acad. Sci. USA*, **97**, 2567–2572.
16. Velasco, A. and Hidalgo, J. (1987) Light and electron microscopical localization of concanavalin A lectin binding sites in rat epiphyseal chondrocytes. *Histochem. J.*, **19**, 7–14.
17. Peterson, A.J., Lindau-Shepard, B., Brumberg, H.A. and Dias, J.A. (2000) Human follicle stimulating hormone receptor variants lacking transmembrane domains display altered post-translational conformations. *Mol. Cell. Endocrinol.*, **160**, 203–217.
18. Panchuk-Voloshina, N., Haugland, R.P., Bishop-Stewart, J., Bhalgat, M.K., Millard, P.J., Mao, F., Leung, W.Y. and Haugland, R.P. (1999) Alexa dyes, a series of new fluorescent dyes that yield exceptionally bright, photostable conjugates. *J. Histochem. Cytochem.*, **47**, 1179–1188.
19. Tinel, H., Cancela, J.M., Mogami, H., Gerasimenko, J.V., Gerasimenko, O.V., Tepikin, A.V. and Petersen, O.H. (1999) Active mitochondria surrounding the pancreatic acinar granule region prevent spreading of inositol trisphosphate-evoked local cytosolic Ca(2+) signals. *EMBO J.*, **18**, 4999–5008.
20. Teasdale, R.D. and Jackson, M.R. (1996) Signal-mediated sorting of membrane proteins between the endoplasmic reticulum and the Golgi apparatus. *Annu. Rev. Cell. Dev. Biol.*, **12**, 27–54.
21. Gabreels, B.A., Swaab, D.F., de Kleijn, D.P., Dean, A., Seidah, N.G., Van de Loo, J.W., Van de Ven, W.J., Martens, G.J. and Van Leeuwen, F.W. (1998) The vasopressin precursor is not processed in the hypothalamus of Wolfram syndrome patients with diabetes insipidus: evidence for the involvement of PC2 and 7B2. *J. Clin. Endocrinol. Metab.*, **83**, 4026–4033.
22. McGeer, P.L., Kawamata, T. and McGeer, E.G. (1998) Localization and possible functions of presenilins in brain. *Rev. Neurosci.*, **9**, 1–15.
23. Nakagawa, T., Zhu, H., Morishima, N., Li, E., Xu, J., Yankner, B.A. and Yuan, J. (2000) Caspase-12 mediates endoplasmic-reticulum-specific apoptosis and cytotoxicity by amyloid-beta. *Nature*, **403**, 98–103.
24. Swift, M. and Swift, R.G. (2000) Psychiatric disorders and mutations at the Wolfram syndrome locus. *Biol. Psychiatry*, **47**, 787–793.
25. Swift, R.G., Perkins, D.O., Chase, C.L., Sadler, D.B. and Swift, M. (1991) Psychiatric disorders in 36 families with Wolfram syndrome. *Am. J. Psychiatry*, **148**, 775–779.
26. Oka, Y., Asano, T., Shibasaki, Y., Kasuga, M., Kanazawa, Y. and Takaku, F. (1988) Studies with antipeptide antibody suggest the presence of at least two types of glucose transporter in rat brain and adipocyte. *J. Biol. Chem.*, **263**, 13432–13439.
27. Ohtsuka, K., Utsumi, K.R., Kaneda, T. and Hattori, H. (1993) Effect of ATP on the release of hsp 70 and hsp 40 from the nucleus in heat-shocked HeLa cells. *Exp. Cell Res.*, **209**, 357–366.
28. Shinoda, K., Mori, S., Ohtsuki, T. and Osawa, Y. (1992) An aromatase-associated cytoplasmic inclusion, the 'stigmoid body', in the rat brain: I. Distribution in the forebrain. *J. Comp. Neuron*, **322**, 360–376.
29. Inoue, H., Nomiyama, J., Nakai, K., Matsutani, A., Tanizawa, Y. and Oka, Y. (1998) Isolation of full-length cDNA of mouse PAX4 gene and identification of its human homologue. *Biochem. Biophys. Res. Commun.*, **243**, 628–633.